The characterization of the water vapor feedback dynamics in Climate Change using a 0D model

Stéphane Hallegatte*
Centre International de Recherche sur l'Environnement et le Développement
and Centre National de Recherche Météorologique, Météo-France
Alain Lahellec, Jean-Yves Grandpeix
Laboratoire de Météorologie Dynamique

April 16, 2004

Abstract

The feedback concept has been used by several authors in the climatology field to comprehensively describe model behaviors and to separate different mechanisms. Here, a global model of climate has been built to analyze the water vapor feedback, making use of elementary laws and parameterizations as determined by GCM results of CO_2 doubling experiments. Beyond a static quantification of the water feedback, an effort to characterize the dynamics of the feedback has been carried out, without loosing the rigorousness of the formal definition of the feedback gain concept.

Two conclusions are drawn: (i) The water vapor effect is found to have a feedback gain of $38\,\%$ (1.6 factor), comparable with results from GCM analyses, but with a very long characteristic time of 8 years. (ii) The water vapor feedback is found negative for time scales below 4 years and positive for longer time scales. This suggests that the water vapor feedback could reduce the natural variability over short time scales while enhancing it on longer time scales. A feedback process does not only influence the equilibrium state, but is rather a dynamic process responsible for transient trajectory modifications.

1. Introduction

The feedback concept is currently used by several authors in the climatology field to characterize the behavior of complex models. Although conceptually meaningful, the practical determination

*corresponding author (hallegatte@centre-cired.fr), CIRED, 45bis Av de la Belle Gabrielle F-94736 Nogent-sur-Marne, FRANCE, tel:(33) 1 43 94 73 74, fax:(33) 1 43 94 73 70

of feedback gains from complex simulation models is far from direct. The numerical treatment of three dimensional equation systems expressing the physical laws and the approximation of sub-grid processes have the consequence to obscure physical paths of the climate processes. For example, the atmospheric humidity is linked to clouds, whose radiative properties are depending on the evolution of the atmospheric water vapor, water droplets and ice particles. It is not easy to separate clouds effect from pure water vapor feedback in the response to forcing changes.

Another difficulty in the interpretation of feedback processes arises from the tempo of the different responses. Some processes participating to the feedback loop may be fast, some others very slow. The usual answer to this problem is to analyze the new equilibrium reached by the system after a perturbation has been applied. This current practice might hide important dynamical components of the response, especially when the forcing is a complex time varying function.

As an introduction to these problems, we first recall in the following section **2.** the current definitions of the feedback gain concept and how they are related to individual climate processes. In section **3.**, a simple model for the water vapor feedback loop of the atmosphere is introduced, as it is supporting our illustration of the feedback methodology in the sequel. We show in section **4.** a direct extension of the feedback concept to include the dynamical characteristics of a climate response to forcing. In section **5.**, the model is used to analyze the dynamical features sustaining the water vapor feedback. The results are summarized in the final section and remaining difficulties concerning the application of feedback loop to complex systems are discussed.

2. The feedback gain concept in its application to climate

The feedback gain concept was introduced by Bode (1945) to characterize the response of linear electric circuit to input signals. The concept is nowadays tentatively applied to climate, although climate models are non linear. The underlying assumption, suggested by the results of Goodman and Marshall (2003), is that as soon as all non linear transients have died, the more inert processes of climate are responding linearly to a moderate amplitude of the forcing change. The feedback gain have proved to be a very useful concept to built comprehensive interpretation of the climate behavior when applied to global circulation models. Hansen et al. (1984), among others, analyze the climate sensitivity in terms of leading feedback mechanisms. Hansen, as well as Bode, uses the following definitions: a feedback is characterized by its gain (g) or its factor (f), defined by:

$$(1-g)\cdot\delta\varphi_1^\infty = \frac{1}{f}\cdot\delta\varphi_1^\infty = \delta\varphi_1^0 \tag{1}$$

where $\delta\varphi_1^\infty$ is the change in equilibrium value of φ_1, after a forcing perturbation has been applied; $\delta\varphi_1^0$ is the change in the equilibrium value of φ_1 for the same perturbation but when the feedback is inoperative. Hence the usual feedback gain definition uses differences between two equilibrium values, and will be hereafter called the *static gain*.

Another approach, used by Coakley (1977) or Wetherald and Manabe (1988), has the advantage of detailing the intervening elementary processes in the loop. To assess the role of a set of feedbacks in the response to a change (ΔF) in the incoming flux (F), they use the partial derivatives of the outgoing flux (R) with respect to the variable involved in each feedback (x_i, i=1,...,n) and the full derivatives of each involved internal variable with respect to the mean surface temperature (T_s). Because the incoming and outgoing fluxes are equal at equilibrium, a relationship

between the incoming flux perturbation and the equilibrium mean surface temperature is obtained:

$$\Delta F = \Delta R \quad \Rightarrow \quad \Delta F = \left(\frac{\partial R}{\partial T_s} + \sum_i \frac{\partial R}{\partial x_i} \frac{dx_i}{dT_s} \right) \Delta T_s \tag{2}$$

By dividing this equation by $\partial R / \partial T_s$, Eq. (2) can be rewritten in the form of Eq. (1):

$$\frac{\overbrace{\Delta F}^{\delta\varphi_1^0}}{\frac{\partial R}{\partial T_s}} = \left(1 + \sum_i \frac{\overbrace{\frac{\partial R}{\partial x_i} \frac{dx_i}{dT_s}}^{-g_i}}{\frac{\partial R}{\partial T_s}} \right) \overbrace{\Delta T_s}^{\delta\varphi_1^\infty} \tag{3}$$

This method has also been extended by Colman et al. (1997) to account for second order derivatives and give an idea of the non-linearity of the processes.

As a first constraint on the practical application of this formulation, the perturbation to the system must go through T_s exclusively, and may not influence directly any other variable. In the case of climate change, considering a CO_2 concentration perturbation with this formalism necessitates to assume that a CO_2 change impacts only upon the surface temperature (which may modify the lapse rate) but does not impact directly upon the lapse rate. A second implication of the given definition relates to the addition of individual feedback gain to determine a complete response of climate through different mechanisms. The full derivative factor in Eq. (3) participating in an individual gain g_i must not include in common processes between the different g_is. It may be difficult in practice to separate these different components of a response in models, as quoted for instance by Schneider et al. (1999).

Both feedback definitions consider equilibrium states and yield purely static gains. We shall introduce a dynamical definition of the feedback concept illustrated with a simple model of a climate feedback loop that we now describe.

3. The Model

The model is mainly built to reproduce water vapor feedback dynamics. As a consequence, other physical processes than radiative transfer are crudely reproduced. After presenting the main assumptions, we introduce our specific formal treatment of the model equations that will be used to generalize the definition of feedback.

a. Description

A single column of atmosphere, containing only water vapor, CO_2 and three cloud layers is considered. Figure 1 displays a schematic diagram of the model. Crude assumptions are applied : (i) convection is not explicitly modeled but its effects are taken into account by fixed lapse rates. This can be justified by Zhang et al. (1994), who showed that variation in lapse rate does not alter significantly the water vapor feedback ; (ii) the ocean mixed layer depth is fixed; (iii) stratosphere SW absorption is fixed; (iv) no ventilation influence on evaporation is considered, although Bates (2003) suggests that it has significant effects; (v) no explicit cloud cover modeling is introduced.

The atmospheric water vapor content is controlled by evaporation and precipitation. Evaporation depends on surface air and ocean temperatures. Precipitation is modeled as a process driving the relative humidity toward a *target relative humidity*, which is supposed to be fixed independently of the CO_2 concentration. This is justified by Hall and Manabe (2000a), who showed that the precipitation annual-mean is controlled by the evaporation annual-mean, and by the classical assumption of constant relative humidity (see IPCC (2001), chp.7 or Hansen et al. (1984)). The target relative humidity is set to 0.7 at surface level, and the characteristic time of the process is set to five days, equal to the synoptic characteristic time. In consequence, the absolute humidity is only controlled by the atmosphere temperature change, with a five-day delay.

The radiative module is a 65-layer column model of the atmosphere, with three cloud layers and two gases (H_2O and CO_2). It computes the LW radiative budgets of the troposphere, stratosphere and ocean, using a Malkmus narrow-band model with a water vapor continuum. The principles behind this module were explored by Green (1967) and developed later by Cherkaoui et al. (1996). Radiative modules based on these principles were built by Hartmann et al. (1984) and Soufiani et al. (1985), who also created the radiation band coefficients tables.

To allow to introduce the dynamic feedback analysis, the model is built according to specific prescriptions, following the Transfer Evolution Formalism (TEF, described below)

b. The Transfer Evolution Formalism Prescriptions

The TEF is a mathematical tool for system analysis and simulation (see Appendix A for a more detailed description). The model presented in the previous section is mathematically represented by a set of equations corresponding to two kinds objects:

1. cells (described in Tab. 1) which are elementary models and correspond to state equations such as:

$$\left\{ \begin{array}{rcl} \frac{\partial \boldsymbol{\eta}_\alpha}{\partial t} & = & \mathbf{G}_\alpha(\boldsymbol{\eta}_\alpha, \boldsymbol{\varphi}_1, \boldsymbol{\varphi}_2, ...) \\ \frac{\partial \boldsymbol{\eta}_\beta}{\partial t} & = & \mathbf{G}_\beta(\boldsymbol{\eta}_\beta, \boldsymbol{\varphi}_1, \boldsymbol{\varphi}_2, ...) \\ ... & & \end{array} \right. \tag{4}$$

   $\boldsymbol{\eta}_\alpha$ is the state variables vector of cell α and the $\boldsymbol{\varphi}_i$ represent the dependent boundary conditions, *i.e.* the variables considered as boundary conditions by a cell, depending upon the complete model state. This dependent boundary conditions are required to make the cells correspond to well-posed problems.

2. transfers (described in Tab. 2 and 3) which are determined by constraint equations such as:

$$\left\{ \begin{array}{rcl} \boldsymbol{\varphi}_1 & = & \mathbf{f}_1(\boldsymbol{\eta}_\alpha, \boldsymbol{\eta}_\beta, ..., \boldsymbol{\varphi}) \\ \boldsymbol{\varphi}_2 & = & \mathbf{f}_2(\boldsymbol{\eta}_\alpha, \boldsymbol{\eta}_\beta, ..., \boldsymbol{\varphi}) \\ ... & & \end{array} \right. \tag{5}$$

Let also $\boldsymbol{\eta}$ be the state vector of the complete system and $\boldsymbol{\varphi}$ be the vector of the full dependent boundary conditions. When initial conditions are given at time t_0, the system is a well-posed problem.

To solve the system, for each time step, the differential of the dynamical system is built around its current state ($\eta(t_n)$) by writing $\eta(t) = \eta(t_n) + \delta\eta(t)$ and $\varphi(t) = \varphi(t_n) + \delta\varphi(t)$. This leads to

the Tangent Linear System (TLS) of the model around the current state:

$$\left\{ \begin{array}{c} \frac{\partial \mathring{\boldsymbol{\delta}}\boldsymbol{\eta}_\alpha(t)}{\partial t} = \mathbf{G}_\alpha|_{t_n} + \underline{\underline{\frac{\partial G_\alpha}{\partial \eta_\alpha}}}\Big|_{t_n} \mathring{\boldsymbol{\delta}}\boldsymbol{\eta}_\alpha(t) + \underline{\underline{\frac{\partial G_\alpha}{\partial \varphi}}}\Big|_{t_n} \mathring{\boldsymbol{\delta}}\boldsymbol{\varphi}(t) \\ \mathring{\boldsymbol{\delta}}\boldsymbol{\varphi}(t) = \sum_\beta \underline{\underline{\frac{\partial f}{\partial \eta_\beta}}}\Big|_{t_n} \mathring{\boldsymbol{\delta}}\boldsymbol{\eta}_\beta(t) + \underline{\underline{\frac{\partial f}{\partial \varphi}}}\Big|_{t_n} \mathring{\boldsymbol{\delta}}\boldsymbol{\varphi}(t) \end{array} \right. \tag{6}$$

It is proved in Appendix A that the Borel transform of this TLS can be written as:

$$\left\{ \begin{array}{rcl} \mathcal{B}[\mathring{\boldsymbol{\delta}}\boldsymbol{\eta}](\tau) & = & \mathcal{B}[\mathring{\boldsymbol{\delta}}\boldsymbol{\eta}_{dec}](\tau) + \underline{\underline{\mathcal{F}}}(\tau)\, \mathcal{B}[\mathring{\boldsymbol{\delta}}\boldsymbol{\varphi}](\tau) \\ \mathcal{B}[\mathring{\boldsymbol{\delta}}\boldsymbol{\varphi}](\tau) & = & \left[1 + \underline{\underline{\mathcal{C}}}(\tau)\right]^{-1} \mathcal{B}[\mathring{\boldsymbol{\delta}}\boldsymbol{\varphi}_{ins}](\tau) \end{array} \right. \tag{7}$$

where $\mathcal{B}[f](\tau)$ is the Borel transform of f(t); τ is the Borel variable; $\mathring{\delta}\eta(t)$ and $\mathring{\delta}\varphi(t)$ are the solutions of the TLS; and where the quantities $\mathring{\boldsymbol{\delta}}\boldsymbol{\eta}_{dec}$, $\underline{\underline{\mathcal{F}}}$, $\underline{\underline{\mathcal{C}}}$, $\mathring{\boldsymbol{\delta}}\boldsymbol{\varphi}_{ins}$ can be calculated from the elementary Jacobian matrices and vectors at time t_n.

All numerical results are obtained with a software developed by the authors and colleagues to implement models expressed with the TEF. An approximation of the step-by-step evolution of the complete system is obtained by solving the system (7) thanks to the approximations:

$$\begin{array}{rcl} \boldsymbol{\delta}\boldsymbol{\eta} & \approx & 2\mathcal{B}[\mathring{\boldsymbol{\delta}}\boldsymbol{\eta}](\frac{\delta t}{2}) \\ \boldsymbol{\delta}\boldsymbol{\varphi} & \approx & 2\mathcal{B}[\mathring{\boldsymbol{\delta}}\boldsymbol{\varphi}](\frac{\delta t}{2}) \end{array} \tag{8}$$

where $\boldsymbol{\delta}\boldsymbol{\eta}$ and $\boldsymbol{\delta}\boldsymbol{\varphi}$ are the state and transfer variable variations in the complete model during a time step δt.

c. Implementation of the model under the TEF

Under the TEF, the system is composed of five sub-systems (5 cells) listed in Tab. 1, together with their state variables and equations. The connections between these sub-systems are represented by 8 "transfer" models (14 transfer variables), listed in Tab. 2 and 3. Parameters are set as given in Tab. 4 and 5. The role of the temperature T_{WV} is detailed in section **4.**.

All cell equations and most of the transfer equations are linear. In this model radiation transfers are weakly non-linear. True non-linearities occur in water vapor equations (evaporation and precipitation).

d. Validation of the model

Table 6 shows LW flux exchanged between the different components of the climate system at the 330 ppm equilibrium. The values are close enough to the observed ones (see Salby (1996), p. 43) to assume that the LW radiative module is able to reproduce realistic budgets. One should mention that the other exchanged fluxes (not shown) are also close to observed values in complex models, showing that the important mechanisms are operating within the simple model.

Table 7 shows the instantaneous partial derivatives of each LW flux with respect to the CO_2 concentration (with all the other variables unchanged), expressed as equivalent CO_2-doubling flux changes. One main observation is a total increase of the Outgoing Long-wave Radiation (OLR): more CO_2 cools down the atmosphere. More precisely, the stratosphere cools down strongly; the troposphere and the ocean warm up slightly. This is a classically found behavior, as quoted in IPCC (2001) (Chp. 2) or Hu and Tung (2002).

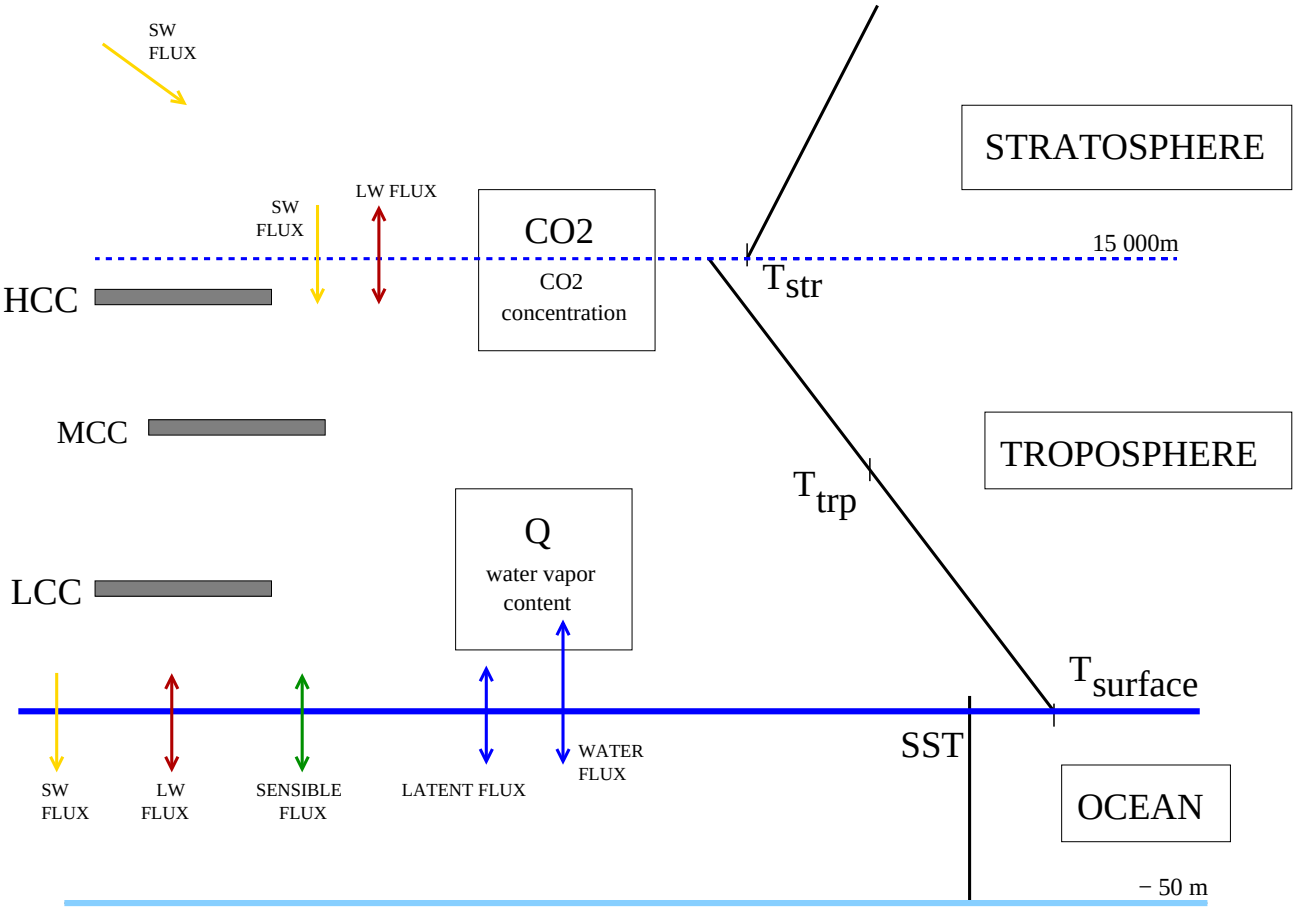

Figure 1: Schematic diagram of the model

Sub-system	State variable	Model
Stratosphere	Average temperature (T_{str}) (K)	Capacitance with fixed and uniform lapse rate $C_p^{str} \cdot \frac{dT_{str}}{dt} = \phi_{SW,str} + \phi_{LW,str}$
Troposphere	Average temperature at 5000m (T_{trp}) (K)	Capacitance with fixed and uniform lapse rate $C_p^{trp} \cdot \frac{dT_{trp}}{dt} = \phi_{SW,trp} + \phi_{LW,trp} + \phi_{sensible,trp} + \phi_{latent,trp}$
Ocean mixed layer	Temperature (SST) (K)	Capacitance with uniform temperature $C_p^{oce} \cdot \frac{dSST}{dt} = \phi_{SW,oce} + \phi_{LW,oce} + \phi_{sensible,oce} + \phi_{latent,oce}$
Water vapor	Water vapor content (Q) ($kg \cdot m^{-2}$)	Capacitance with fixed relative humidity gradient (γ_r) $\frac{dQ}{dt} = \frac{1}{L_{ve}} \cdot (-\phi_{latent,oce} - \phi_{latent,trp})$
Carbon dioxyde	CO_2 concentration (CO_2) (ppmv)	Fixed

Table 1: Model sub-systems with state variables and model types

Transfer	Transfer variable(s)	Model
Solar flux	SW budget of troposphere, stratosphere, ocean ($\phi_{SW,trp}$, $\phi_{SW,str}$, $\phi_{LW,oce}$) ($W \cdot m^{-2}$)	constant solar flux shared between ocean, troposphere, stratosphere and reflected flux to space $\phi_{SW,str} = 40\ W \cdot m^{-2}$ $\phi_{SW,trp} = (1 - a_{cloud}) \cdot C \cdot F_{SW}$ $\phi_{SW,oce} = (1 - albedo) \cdot (1 - C) \cdot F_{SW}$ $C = 1 - (1 - \alpha_{SW}^{L} \cdot LCC) \cdot (1 - \alpha_{SW}^{M} \cdot MCC) \cdot (1 - \alpha_{SW}^{H} \cdot HCC)$
LW flux	LW budget of troposphere, stratosphere, ocean ($\phi_{LW,trp}$, $\phi_{LW,str}$, $\phi_{LW,oce}$) ($W \cdot m^{-2}$)	Malkmus narrow-band radiative module
Sensible heat flux	Surface heat flux ($\phi_{sensible,trp}$) ($W \cdot m^{-2}$)	Diffusive term proportional to surface temperature difference $\phi_{sensible,trp} = -\phi_{sensible,oce} = h_{cond} \cdot (SST - T_{surf})$ $T_{surf} = T_{trp} - \gamma_{trp} \cdot H_{moy}$

Table 2: Transfer models, with transfer variables and model types (Part I)

Transfer	Transfer variable(s)	Model
Precipitation	Surface precipitation and corresponding latent heat flux ($\phi_{latent,trp}$) ($W \cdot m^{-2}$)	Newtonian term nudging tropospheric relative humidity toward target relative humidity $\phi_{latent,trp} = -\phi_{latent,oce} + L_{ve} \cdot \frac{1}{\tau_P} \cdot (Q - Q^{\infty}(T_{trp}))$ $Q^{\infty}(T_{trp})$ is the water vapor content corresponding to the target relative humidity.
Evaporation	Surface latent heat flux ($\phi_{latent,oce}$) ($W \cdot m^{-2}$)	Diffusive term proportional to surface humidity difference $\phi_{latent,oce} = k_{evap} \cdot L_{ve} \cdot (P_{sat}(SST) - r_H \cdot P_{sat}(T_{surf}))$ $P_{sat}(T)$ is the water vapor saturation pressure.
WV temperature	T_{WV} (K)	$T_{WV} = T_{trp}$
Cloud cover	High, medium and low level cloud cover (HCC, MCC, LCC) (no unit)	fixed: $HCC = HCC_0$, $MCC = MCC_0$ $LCC = LCC_0$

Table 3: Transfer models, with transfer variables and model types (Part II)

Variable	Value
Surface relative humidity at equilibrium	0.7
Top of the atmosphere altitude	65,000m
Tropopause altitude	15,000m
Mean troposphere altitude (H_{moy})	5000 m
Troposphere lapse rate (γ_{trp})	$-6.5 \cdot 10^{-3}\ Km^{-1}$
Troposphere heat capacity (C_p^{trp})	$1. \cdot 10^{7}\ J \cdot K^{-1} \cdot m^{-2}$
Stratosphere lapse rate (γ_{str})	$3.5 \cdot 10^{-3}\ Km^{-1}$
Stratosphere heat capacity (C_p^{str})	$1.2 \cdot 10^{6}\ J \cdot K^{-1} \cdot m^{-2}$
Cloud albedo (a_{cloud})	0.88
High level cloud cover (HCC_0)	0.35
High level cloud altitude	14,000m
High level cloud SW absorption (α_{SW}^H)	0.3
High level cloud emissivity	1.
Mean level cloud cover (MCC_0)	0.25
Mean level cloud altitude	6,000m
Mean level cloud SW absorption (α_{SW}^M)	1.
Mean level cloud emissivity	1.
Low level cloud cover (LCC_0)	0.30
Low level cloud altitude	2,000m
Low level cloud SW absorption (α_{SW}^L)	1.
Low level cloud emissivity	1.

Table 4: Atmosphere parameter values

Variable	Value
Ocean albedo ($albedo$)	0.05
Ocean heat capacity (C_p^{oce})	$2. \cdot 10^8\ J \cdot K^{-1} \cdot m^{-2}$
Oceanic mixed layer thickness	50m
Atmosphere-Ocean sensible heat transfer coefficient (h_{cond})	$1.4\ W \cdot m^{-2} \cdot K^{-1}$
Evaporation coefficient (k_{evap})	$0.7 \cdot 10^{-2}\ s \cdot m^{-1}$
Precipitation characteristic time (τ_p)	5 days
Latent heat of evaporation (L_{ve})	$2.5 \cdot 10^6\ J \cdot kg^{-1}$
Incoming solar flux (F_{SW})	$340\ W \cdot m^{-2}$

Table 5: Surface parameter values

Emitters LW	Absorption ($W \cdot m^{-2}$)			
	Ocean	Space	Tropo.	Strato.
Ocean	•	27.3	363.1	0.3
Space	0.	•	0.	0.
Troposphere	329.7	131.5	•	19.9
Stratosphere	0.1	48.1	12.9	•

Table 6: LW cloudy sky exchanged fluxes. Each line shows the flux emitted by an object to the others. Each column shows the flux absorbed by an object. The sum of the ocean column is the total LW flux absorbed by the ocean. The sum of the Ocean line is the total LW flux emitted by the ocean. The total OLR is $207\ W \cdot m^{-2}$

Another observation is the increase in the LW flux emitted by ocean and absorbed by stratosphere: the absorption effect of the larger amount of CO_2 in stratosphere is slightly overriding the additional screening effect of the tropospheric CO_2. Figure 2 shows the time evolution of state variables, in response to a step from 330 ppm to 660 ppm in CO_2 concentration. On the stratospheric time scale, troposphere and ocean temperatures are almost constant. Consequently, the stratosphere reaches a quasi-equilibrium corresponding to its new CO_2 concentration and to the tropospheric and oceanic initial temperatures. This corresponds to the standard definition of additional CO_2 radiative forcing. The results from the model (e.g. at the doubled CO_2 concentration, $F_{2X} = 3.3\,W \cdot m^{-2}$) are fairly close to those of other studies (IPCC (2001), Chp. 6).

On longer time scales, the troposphere and ocean warm up slightly, and the stratosphere, always at radiative quasi-equilibrium, begins to warm up slowly. Nevertheless, the final effect on the stratosphere is a strong cooling, since the initial stratosphere cooling is much larger than the subsequent warming.

Table 8 shows the equilibrium values of the state variables for various CO_2 concentrations (the model never shows instability). The climate sensitivity of the model to doubling CO_2 concentration is +1.1 K. This is low compared with most of GCM results (see IPCC (2001), Chp.9 or Kothavala et al. (1999)). It may be mainly explained by (i) the non-dependency of the cloud cover on the temperature and water vapor content; (ii) the lack of ice, snow, and lapse rate feedbacks. This underestimation of the warming is not a critical problem since our aim is not to provide numerical estimates of the variables but to carry out a dynamical analysis of some selected processes.

Emission LW	Absorption derivative($W \cdot m^{-2} \cdot 330\, ppmv^{-1}$)			
	Ocean	Space	Tropo.	Strato.
Ocean	•	-3.2	3.0	0.2
Space	0.	•	0.	0.
Troposphere	3.0	-5.1	•	2.6
Stratosphere	0.	13.9	1.6	•

Table 7: Instantaneous derivative of exchanged fluxes with respect to the CO_2 concentration (expressed in equivalent CO_2-doubling flux changes).

CO_2 (ppmv)	Δ Equilibrium Temperatures (K)			Δ water vapor content ($kg \cdot m^{-2}$)
	Ocean	Surface air	Tropopause	
110	-1.1	-1.3	+0.9	-2.3 (-9 %)
330	0.0	0.0	0.0	0.0
660	+0.9	+1.1	-5.0	+2.0 (+7 %)
1320	+2.1	+2.5	-9.5	+4.8 (+18 %)
2640	+3.6	+4.4	-13.6	+8.9 (+33 %)

Table 8: Equilibrium state variables values from different CO_2 concentrations

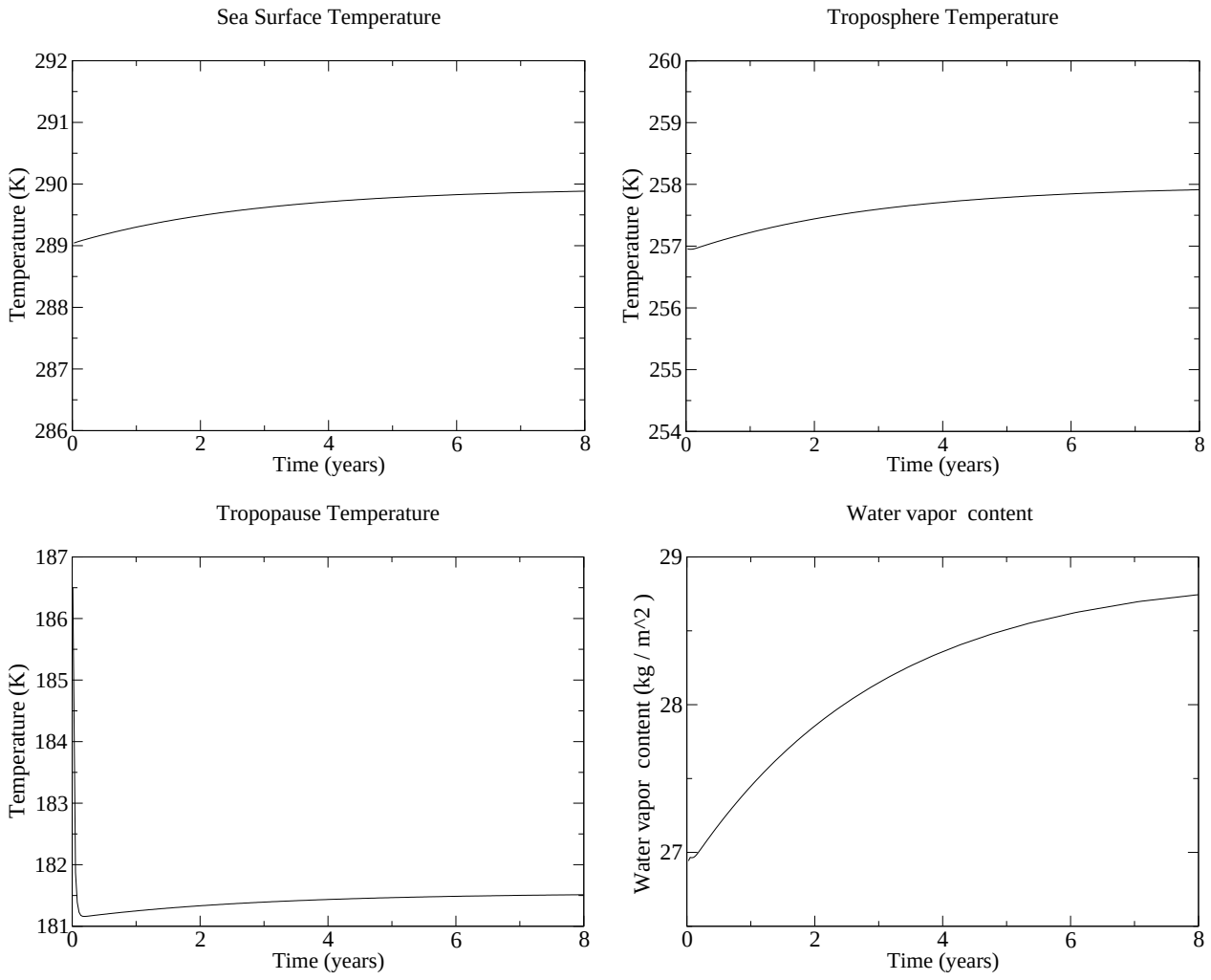

Figure 2: Dynamical response of the model to a step in CO_2 concentration: (a) upper left: sea surface temperature; (b) upper right: troposphere temperature, at 5000m; (c) lower left, tropopause temperature; (d) lower right, water vapor content ($kg \cdot m^{-2}$)

4. Methodology for feedback study

a. Feedback definition and static characterization

Within the TEF, a feedback loop is defined as a set of processes interfaced by transfer variables $\{\delta\varphi_i$,i=1,..,n$\}$ in which the evolution of each variable $\delta\varphi_j$ depends only on $\delta\varphi_{j-1}$ (and the evolution of $\delta\varphi_1$ depends only on $\delta\varphi_n$).

This definition is coherent with the terminology recalled in section **2.** for static gain. Because the trajectory from one equilibrium to another is a key issue to understand the mechanisms underlying a feedback and its interaction with other processes, a feedback characterization which describes the whole dynamics of the response is needed. The TEF implementation of models allows to take into account the involved dynamics.

b. Feedback loop dynamics

In order to analyze the dynamics of feedback loops, the model TLS is analyzed. Since the system is non-linear, the TLS evolves with time. We will thus illustrate the concept using a stable equilibrium state of the system where the TLS allows to implicitly analyze perturbed trajectories. This means we leave aside the important problem of dealing with non linear systems out of equilibrium.

As far as concerning perturbations of the model at stable equilibrium state, the TLS is valid without time limit and is able to describe the complete model response dynamics to small perturbations.

Once a model described within the TEF, the method to extract a specific feedback loop from the system is straightforward: it consists in eliminating all variables except one, say $\mathring{\delta}\varphi_1$, in the algebraic system (7). The remaining scalar equation reads :

$$(1 - g_1(\tau)) \cdot \mathcal{B}[\mathring{\delta}\varphi_1](\tau) = \mathcal{B}[\mathring{\delta}\varphi_{1_{ins}}'](\tau) \tag{9}$$

It is shown in Appendix A that $\mathring{\delta}\varphi'_{1,ins}$ is the φ_1 variation when the rest of the system (all of the eliminated variables) is insensitive to a change in φ_1 (in other terms: when the open loop is obtained by a cut just after the φ_1 path in Fig. 3). We define $g_1(\tau)$ as *the dynamic gain of the feedback* because it represents the effect of closing the feedback loop: perturbation on $\varphi_1 \rightarrow$ perturbation impacts on the rest of the system $\rightarrow$ further perturbation on φ_1.

Note that the function $g_1(\tau)$ generalizes the concept of feedback gain, since at the infinite limit:

$$\lim_{t\to+\infty} \mathcal{B}^{-1}[g_1(\tau)](t) \quad = \quad \lim_{\tau\to+\infty}[g_1(\tau)] \quad = \quad g \qquad \text{(static gain)} \tag{10}$$

Where the feedback static gain gives only the response corresponding to an asymptotic behavior (the new equilibrium value), the feedback dynamic gain describes the whole response dynamics of $\mathring{\delta}\varphi_1$, and hence the whole dynamics of the feedback, through the inverse Borel transform of Eq. (9) rewritten as:

$$\mathring{\delta}\varphi_1(t) = \mathcal{B}^{-1}\left[\frac{1}{1 - g_1(\tau)}\right] * \frac{d}{dt}\mathring{\delta}\varphi_{1_{ins}}(t) \tag{11}$$

This equation shows that $\mathcal{B}^{-1}[1/(1 - g_1(\tau))]$ links the model dynamics when the loop is open ($\mathring{\delta}\varphi_{1_{ins}}(t)$) to the model dynamics when the loop is closed ($\mathring{\delta}\varphi_1(t)$).

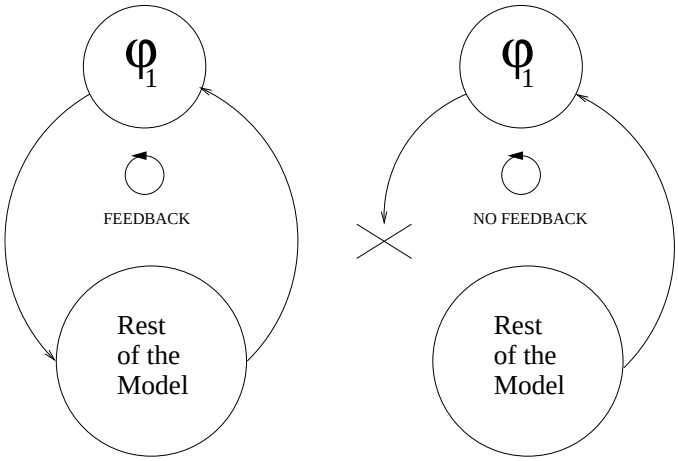

Figure 3: Scheme of a feedback (left) and illustration of the open-loop model (right).

5. Application to the water vapor feedback

a. Definition of the water vapor feedback

Our simple model is designed to focus on the Water Vapor (WV) feedback. The model is built in order to implement one among the possible definitions of the water vapor feedback. The loop in the model is the following: a troposphere temperature increase occurs; the relative humidity is decreased (as a consequence of the Clausius-Clapeyron relation); precipitation, modeled to maintain a constant relative humidity, decreases (on the constant relative humidity hypothesis, see Salathé and Hartmann (1997) or Del Genio et al. (1994)); the relative humidity goes back to its initial level, corresponding to a larger total water content; the radiative budget is modified (troposphere and ocean warm up); as a consequence, the troposphere temperature increase is amplified.

However, the troposphere temperature is involved in several feedback loops so that the feedback gain associated to the T variable results from the interplay of many processes. The same type of problem occurs in GCM feedback analysis and explains why it is very difficult to carry out rigorous feedback analysis in GCM (see Schneider et al. (1999)). In particular, cutting the water vapor feedback by replacing, during a CO_2 increase simulation, the humidity by humidity fields calculated in a control simulation raises several problems: in particular, the short-term and low scale consistency between cloud cover and humidity is lost.

In order to have loops involving mechanisms that can be separated, we shall introduce one extra variable: T_{WV}. T_{WV} is supposed to be the temperature which is pertinent to the mechanisms driving the the water vapor. T_{WV} may be for instance the temperature at a given atmosphere level or a temperature modified by some processes. In the model, T_{WV} is taken equal to the atmospheric temperature T. In other terms, T_{WV} is equal to T but does not represent the same thing: it is not the atmosphere temperature, it is the temperature pertinent to water vapor process.

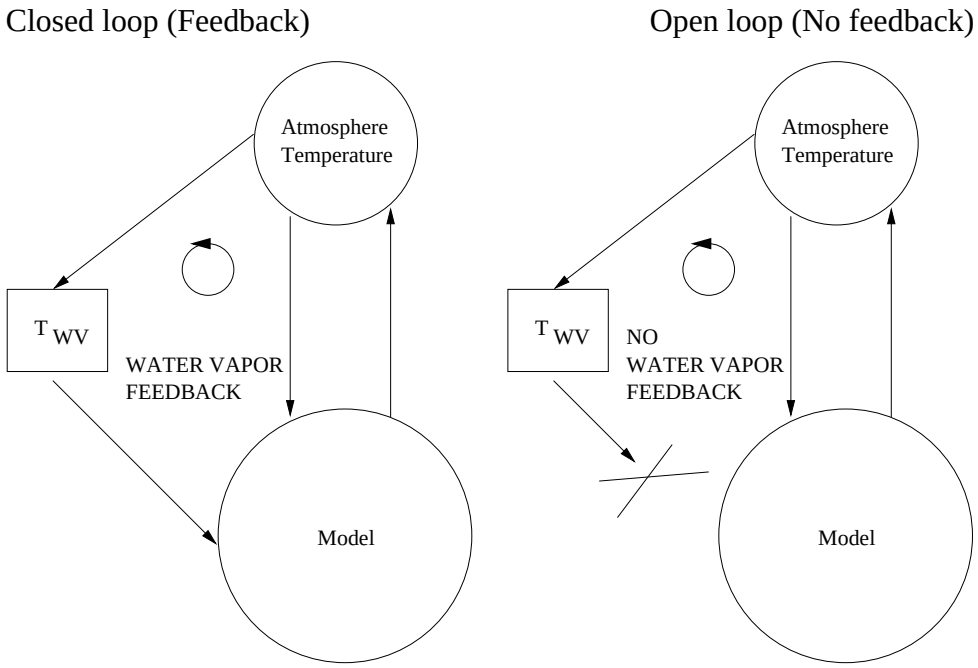

Figure 4: Scheme of the water vapor feedback (left), involving a new temperature variable used by all water vapor processes, when the other processes keep using the initial temperature variable; and illustration of the open-loop model (right).

The introduction of this variable modifies the model equations the following way:

$$\left\{\begin{array}{lcl} T &=& f(\eta, Q) \\ Q &=& F(\eta, T) \\ \eta &=& G(T, Q) \end{array}\right. \longrightarrow \left\{\begin{array}{lcl} T &=& f(\eta, Q) \\ T_{WV} &=& T \\ Q &=& F(\eta, T_{WV}) \\ \eta &=& G(T, Q) \end{array}\right. \tag{12}$$

where T, Q are the sub-models mean troposphere temperature and humidity, and η are all the other variables. Although the two models have the same solution, the feedback loops are different. In the new form of the model, there is a loop going through T_{WV} that is distinct from all other loops going through T. The water vapor loop is now rigorously defined: the water vapor temperature T_{WV} may be perturbed (say by a slight change in altitude if T_{WV} is defined as the temperature at a pertinent level), and may now deviate from the troposphere temperature T. The obtained water vapor feedback loop is shown in Fig. 4. When the loop is open, one may perturb the model and read the response of the system without feedback in T_{WV}. The water vapor feedback gain describes the difference in the response of T to such a perturbation in the open loop and in the closed loop cases. This methodology, akin to the methodology used by Hall and Manabe (2000b) in their GCM feedback analysis, enables us to suppress the water vapor feedback without loosing the water conservation and the model consistency.

b. Characterization of the water vapor feedback

Choosing T_{WV} as the only retained variable in the algebraic elimination process, Eq. (11) becomes:

$$\mathring{\delta}T_{WV}(t) = \mathcal{B}^{-1}\left[\frac{1}{1-g_{WV}(\tau)}\right] * \frac{d}{dt}\mathring{\delta}T_{WV,ins}(t) \tag{13}$$

where $\mathring{\delta}T_{WV}(t)$ and $\mathring{\delta}T_{WV,ins}(t)$ are the variation obtained in the closed loop case and the open loop case respectively (see Fig. 4), and $g_{WV}(\tau)$ is the dynamic gain of the "water vapor feedback".

The expression $(\mathcal{B}^{-1}[(1-g_{WV}(\tau))^{-1}](t)\cdot\Delta T_0)$ may be interpreted as the complete change in $\mathring{\delta}T_{WV}$ after an initial step ΔT_0 is applied, corresponding to the following modification in the equations of (12): $T_{WV} = T$ if $t \leq 0$; and $T_{WV} = T + \Delta T_0$ if $t > 0$). This response includes the perturbing step, i.e. $\mathring{\delta}T_{WV}(t)$ is not continuous at $t = 0$.

In order to keep only the real feedback effect, the *feedback function* is defined as:

$$\mathring{\delta}F_{T_{WV}}(t) = \left(\mathcal{B}^{-1}\left[\frac{1}{1-g_{WV}(\tau)}\right] - 1\right)\cdot(1\ K) \tag{14}$$

which is the T_{WV} feedback function corresponding to the water vapor feedback, i.e. the additional troposphere temperature increase due to the water vapor feedback after perturbing the T_{WV} model by a 1 K step.

In the simple model, the water vapor feedback function reads:

$$\mathring{\delta}F_{T_{WV}}(t) = -0.56\cdot(1-e^{-\frac{t}{\tau_1}}) + 1.17\cdot(1-e^{-\frac{t}{\tau_2}}) \tag{15}$$

with $\tau_1 = 7$ days and $\tau_2 = 7.7$ years. The corresponding response function is shown in Fig. 5.

c. Feedback function Interpretation

We find that the slow and fast poles are linked with the following mechanisms: the fast pole corresponds mainly to the lowering of latent heat flux due to the rainfall decrease, which comes from the rising temperature (*i.e.* corresponding to a decrease in relative humidity). This mechanism is one path of the water vapor feedback: any transient trajectory with an increase in the atmospheric absolute humidity results in an unbalance between precipitation and evaporation and hence necessitates an increase in the atmospheric latent energy content compared with the equilibrium state. In consequence, the water vapor feedback process involves a rapid atmospheric cooling, as assessed by our model, with a time response of about a few days. This negative feedback can be illustrated by considering a doubling-CO_2-experiment which leads to a 3 K surface temperature increase. If relative humidity is constant, the absolute humidity approximately doubles. This corresponds roughly to an addition of $30\,kg\cdot m^{-2}$ of water vapor in the atmosphere, i.e. a latent energy loss of $-8\cdot10^7\,J\cdot m^{-2}$. Because the involved flux changes are about $3\,W\cdot m^{-2}$, 9 months are necessary to reach that energy.

The slow pole corresponds to the true water vapor feedback, i.e. the process by which the atmosphere warms up when an increase in water vapor concentration modifies the LW radiative balance. Equation (15) gives an estimate of 8 years as the characteristic time of that slow pole. This very long characteristic time can be explained by the fact that the water vapor feedback is composed of several non-zero characteristic time processes: an initial temperature perturbation

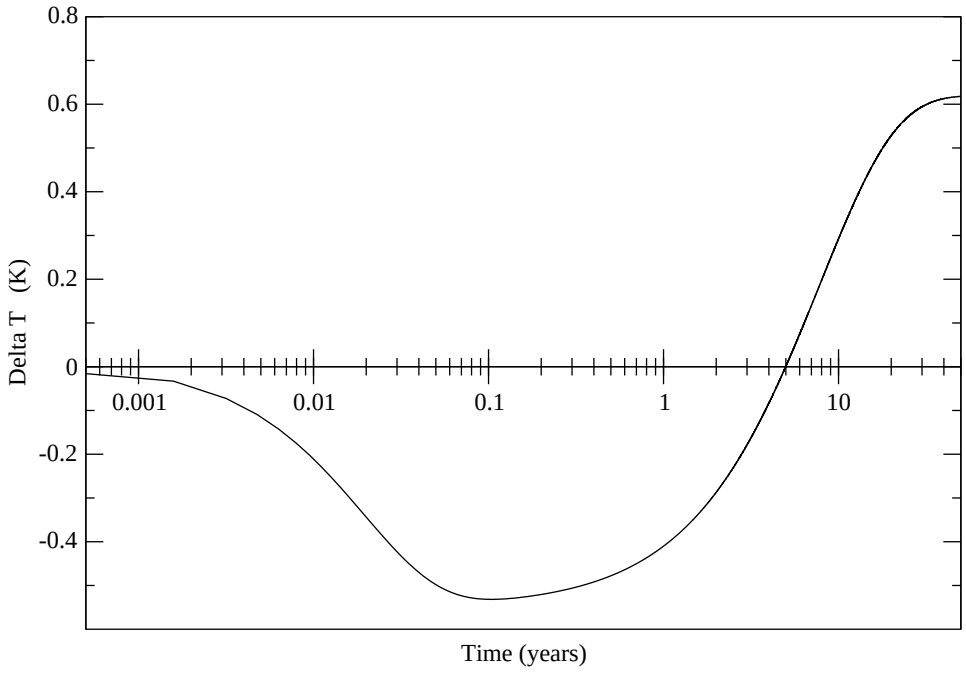

Figure 5: ΔT feedback function of the water vapor feedback. When the temperature is perturbed by a 1 K step at t=0, this function shows the temperature change added to the perturbation, due to the water vapor feedback. We may distinguish two main processes: the cooling due to the temporary decrease in precipitation and the warming due to the definitive increase in absolute humidity.

leads to a progressive increase of the absolute humidity, which causes a progressive temperature increase through the greenhouse effect. This step-by-step process leads to a final temperature increase, and may involve long characteristic times and complex behavior, hidden in the equilibrium approach of static feedback analyzes.

Applying Eq. (10) to Eq. (15) yields the WV feedback static gain $g_{WV} = 38\ \%$. This value is close to the results from GCMs (see Lindzen (1993) and Schneider et al. (1999)). Nevertheless, the elicitation of the fast and negative part of the feedback shows the interest of the methodology: the water vapor feedback is not a continuous and regular process only responsible for enhancing the temperature increase, but is rather a complex dynamic process responsible for a temporal pathway of the temperature change. One consequence of this understanding of the water feedback is discussed now.

d. Influence of a feedback on variability

Since the feedback is now dynamically characterized, it may be interesting to focus on the influence of one feedback on the complete model dynamics. This can be made explicit by considering a feedback and a sinusoidal perturbation starting at $t = 0$, such that the temperature variation is given by Eq. (16) if the feedback is made inoperative.

$$t > 0 \implies \mathring{\delta}T_{WV,ins}(t) = A_0 \cdot sin(\omega t) \tag{16}$$

As shown by Eq. (13), the temperature variations due to this perturbation, now taking into account the feedback, becomes:

$$\mathring{\delta}T_{WV}(t) = (1 + \mathring{\delta}F_{T_{WV}}(t)) * \frac{d}{dt}\mathring{\delta}T_{WV,ins}(t) \tag{17}$$

Assuming that all poles are real, negative and simple, the feedback function $\mathring{\delta}F_{T_{WV}}(t)$ reads:

$$\mathring{\delta}F_{T_{WV}}(t) = \sum_{i=1}^{n} \lambda_i \cdot (1 - e^{-\frac{t}{\tau_i}}) \tag{18}$$

Elementary calculations lead to:

$$\mathring{\delta}T_{WV}(t) = A_0 \left(\overbrace{sin(\omega t)}^{(1)} + \sum_{i=1}^{n} \overbrace{\frac{\lambda_i}{1 + (\tau_i \omega)^2}(sin(\omega t) - \omega \tau_i cos(\omega t))}^{(2)} - \overbrace{\frac{\omega \tau_i \lambda_i}{1 + (\tau_i \omega)^2} e^{-\frac{t}{\tau_i}}}^{(3)} \right) \tag{19}$$

where (1) is the perturbation; (2) is the permanent influence of the pole; (3) is the transient influence of the pole. This shows that, for each feedback pole i:

1. if $\omega^{-1} << \tau_i$, *i.e.* if the perturbation time scale is much shorter than the feedback pole characteristic time, the pole has no influence on the temperature variation;
2. if $\omega^{-1} >> \tau_i$, *i.e.* if the perturbation time scale is much longer than the feedback pole characteristic time, the pole does have an influence on the temperature variation. In that case, the influence of the i^{th} pole leads to the following permanent temperature evolution:

$$\mathring{\delta}T^i_{WV}(t) = A_0(1 + \lambda_i)sin(\omega t) \tag{20}$$

Hence, if such a feedback pole corresponds to a positive feedback, it enhances the oscillation amplitude, thus enhancing the variability. Conversely, a negative feedback pole reduces the variability.

3. Between these extremes, when the feedback pole characteristic time is close to the perturbation time scale, the influence of the feedback pole decreases when the perturbation time scale decreases.

In the case of the water vapor feedback, as assessed in this study, one pole has a 7-days characteristic time and corresponds to a negative feedback; one pole has an 8-year characteristic time and corresponds to a positive feedback. Then, the water vapor feedback should reduce the variability on short time scales, for which the pole corresponding to a negative feedback only may influence the system. The same mechanism also enhances the variability on longer time scales, for which both poles influence the system.

More generally, the dynamics of feedbacks is needed when forcing conditions are varying. In the case of long time scale perturbation, as is the case for the current CO_2 concentration increase, rapid responses are indeed observed and responsible for changes in the transient pathway followed by the climate system.

e. Consequences on the behavior of forced and coupled models

Barsugli and Battisti (1998), in their Fig. 10, found a higher atmosphere temperature variability in coupled GCM than in forced GCM for long-term perturbation (*i.e.* longer than one year). But conversely, **?** found that the atmospheric temperature short term variability is higher in a forced GCM than in a coupled GCM.

These results may be linked to the WV feedback: it is generally accepted that, over the short term, atmosphere is driving the ocean mixed layer. In consequence, running an AGCM forced by SST extracted from a coupled simulation means cutting the short-term and low scale consistency between atmospheric surface temperature and SST. Any short scale feedback involving atmosphere and sea surface is broken in the forced model.

Hence the fast and negative pole of the WV feedback is probably non-operative in a forced AGCM simulation leading to a higher natural variability on the short term than in coupled simulations.

6. Concluding discussion

The analysis presented here uses the Tangent Linear System of the model to study feedback dynamic features. We have shown that the set up of feedbacks is a transient process, and we have introduced a feedback gain function of time (more precisely depending on the Borel variable τ). With this function, important characteristic time of the climate mechanisms can be exhibited. The water vapor feedback, which is found to have a positive static feedback gain of 38%, has a component with a characteristic time close to 8 years. Nevertheless, the Water Vapor feedback is found to be negative for time scales shorter than a few years and to become positive on longer time scales only. This effect, due to the latent flux released by a return to equilibrium of the relative humidity, suggests that the natural variability differences between coupled and forced GCM are

related to the considered time scale. As discussed in section **5.**d., this effect finds a confirmation in the observation of Barsugli and Battisti (1998) and **?**, i.e. an increased short term atmospheric variability of forced GCMs compared to coupled GCMs, and conversely a reduced variability on time scales longer than a few years. This particularity of the response function also stresses that several years delay may be needed before being able to diagnose an effect on climate of a slow CO_2 increase.

This work emphasizes that complex interactions between processes - even if limited here since concerning a simple model - lead to a dynamical complexity of the climate response. While we could associate the slowest characteristic time with the ocean, it is in general difficult to link each elementary process with a time constant. It is also far from trivial to separate the feedback loops in a strict manner. This separation is essential to justify the classical method used for instance by Schneider et al. (1999). The methodology presented here allows to define rigorously the feedback, but it requires to modify the original model.

Our analysis is entirely based on the TLS at equilibrium. There is no evident way to extend the method to non-linear system out of equilibrium, for which the TLS system is non-autonomous. An interesting direction of research is given by Aires and Rossow (2003), which characterize the non-linear system following the non-autonomous TLS as it evolves along a full model trajectory. In that case, the non-linear system is described as histograms of the different TLS coefficients sampled along the trajectory. It is, in theory, possible to extend their method with a dynamical characterization of each TLS coefficient in the histograms, but to obtain a compound propagator of the system, one has to consider the combination of possibly rotating singular vectors of elementary TLS matrices. This leads to severe difficulty and there is still a long way to go before a comprehensive treatment of the climate system.

Another result may justify the TLS approach in a more hypothetical way. Goodman and Marshall (2003) compared the singular elements of the TLS of their MM93 model with the EOFs of the non-linear simulation. They found close analogy between the slowest singular modes and the leading EOFs. This suggest that the slowest response structures to perturbations respond linearly to the quickest (non-linear) synoptic perturbations. If this is correct, the linear slowest response reproduce a realistic long term climate behavior, as long as no bifurcation occurs. This would emphasize the interest of the dynamical characterization of the TLS. These results meet some parallel with ours: we found that a change in the quickest time response of our simple model (5 days for precipitation adjustment) does not significantly modify the values of the slowest modes. It thus appears that the slowest modes are robust, even when the fastest ones are uncertain, suggesting that the inert part of the TLS is autonomous.

7. Acknowledgments

The authors wish to acknowledge METEO-FRANCE for financial support. They thank Olivier Tallagrand and Venance Journé for helpful comments and remarks, and Robert Franchisseur for computer support. The remaining errors are entirely the authors'.

A Appendix: the Transfer Evolution Formalism

a. Tangent Linear System Analysis

As explained in the article, the model is mathematically represented by a set of equations of two kinds:

1. cells:

$$\begin{array}{rcl} \frac{\partial \boldsymbol{\eta}_\alpha}{\partial t} & = & \mathbf{G}_\alpha(\boldsymbol{\eta}_\alpha, \boldsymbol{\varphi}_1, \boldsymbol{\varphi}_2, ...) \\ \frac{\partial \boldsymbol{\eta}_\beta}{\partial t} & = & \mathbf{G}_\beta(\boldsymbol{\eta}_\beta, \boldsymbol{\varphi}_1, \boldsymbol{\varphi}_2, ...) \\ ... & & \end{array} \tag{A-1}$$

2. transfers:

$$\begin{array}{rcl} \boldsymbol{\varphi}_1 & = & \mathbf{f}_1(\boldsymbol{\eta}_\alpha, \boldsymbol{\eta}_\beta, ..., \boldsymbol{\varphi}) \\ \boldsymbol{\varphi}_2 & = & \mathbf{f}_2(\boldsymbol{\eta}_\alpha, \boldsymbol{\eta}_\beta, ..., \boldsymbol{\varphi}) \\ ... & & \end{array} \tag{A-2}$$

Let $\boldsymbol{\eta}$ be the state vector of the complete system and $\boldsymbol{\varphi}$ be the vector of the dependent boundary conditions. With initial conditions at time t_0, the system is a well-posed problem.

The method consists in building the first order development of the dynamical system around its current state ($\eta(t_n)$). For each cell α, it reads:

$$\begin{array}{r} \frac{\partial(\boldsymbol{\eta}_\alpha(t_n)+\boldsymbol{\delta\eta}_\alpha(t))}{\partial t} = G_\alpha(\boldsymbol{\eta}_\alpha(t_n), \varphi(t_n)) + (\underline{\underline{\frac{\partial G_\alpha}{\partial \eta_\alpha}}})(\boldsymbol{\eta}_\alpha(t_n), \varphi(t_n)) \cdot \boldsymbol{\delta\eta}_\alpha(t) \\ +(\underline{\underline{\frac{\partial G_\alpha}{\partial \varphi}}})(\boldsymbol{\eta}_\alpha(t_n), \varphi(t_n)) \cdot \boldsymbol{\delta\varphi}(t) + \mathcal{O}((t-t_n)^2) \end{array} \tag{A-3}$$

where $\boldsymbol{\delta\eta}_\alpha(t) = \boldsymbol{\eta}_\alpha(t) - \boldsymbol{\eta}_\alpha(t_n)$, and $\boldsymbol{\delta\varphi}(t) = \boldsymbol{\varphi}(t) - \boldsymbol{\varphi}(t_n)$.

The Tangent Linear System (TLS) corresponding to system (A-3) is, for each cell α:

$$\left\{ \begin{array}{c} \frac{\partial \mathring{\boldsymbol{\delta}}\boldsymbol{\eta}_\alpha(t)}{\partial t} = \mathbf{G}_\alpha|_{t_n} + \underline{\underline{\frac{\partial G_\alpha}{\partial \eta_\alpha}}}\Big|_{t_n} \mathring{\boldsymbol{\delta}}\boldsymbol{\eta}_\alpha(t) + \underline{\underline{\frac{\partial G_\alpha}{\partial \varphi}}}\Big|_{t_n} \mathring{\boldsymbol{\delta}}\boldsymbol{\varphi}(t) \\ \mathring{\boldsymbol{\delta}}\boldsymbol{\varphi}(t) = \sum_\beta \underline{\underline{\frac{\partial f}{\partial \eta_\beta}}}\Big|_{t_n} \mathring{\boldsymbol{\delta}}\boldsymbol{\eta}_\beta(t) + \underline{\underline{\frac{\partial f}{\partial \varphi}}}\Big|_{t_n} \mathring{\boldsymbol{\delta}}\boldsymbol{\varphi}(t) \end{array} \right. \tag{A-4}$$

where the suffix β sweeps the list of sub-domains.

We approximate the true time evolution of the model ($\boldsymbol{\delta\eta}_\alpha(t)$ and $\boldsymbol{\delta\varphi}(t)$) by $\mathring{\boldsymbol{\delta}}\boldsymbol{\eta}_\alpha(t)$ and $\mathring{\boldsymbol{\delta}}\boldsymbol{\varphi}(t)$, the TLS solutions, since they differ only by $\mathcal{O}((t-t_n)^2)$.

In formulation (A-4), the Jacobian matrices contain critical information for the analysis of the interaction between variables. The TLS can be solved by various methods, including Laplace transforms. Rather than Laplace transformation, we shall use the more convenient Borel transformation defined by:

$$f(t) \overset{\mathcal{B}}{\rightarrow} \mathcal{B}[f](\tau) = \frac{1}{\tau}\int_0^\infty e^{-t/\tau} f(t)dt = \frac{1}{\tau}\widetilde{f}(\frac{1}{\tau}) \tag{A-5}$$

where $\widetilde{f}(p)$ stands for the Laplace transform of $f(t)$. Contrary to the Laplace variable, the Borel variable τ is real and homogeneous to time.

Because $\mathcal{B}[\partial f/\partial t](\tau) = (1/\tau)\mathcal{B}[f](\tau)$, the Borel transform of Eq. (A-4) reads:

$$\left\{ \begin{array}{c} \mathcal{B}[\mathring{\boldsymbol{\delta}}\boldsymbol{\eta}_\alpha](\tau) = \overbrace{\left[1-\tau\ \underline{\underline{\left.\frac{\partial G_\alpha}{\partial \eta_\alpha}\right|_{t_n}}}\right]^{-1}}^{\mathcal{B}[\mathring{\boldsymbol{\delta}}\boldsymbol{\eta}_{\alpha,dec}](\tau)} \tau\ \mathbf{G}_\alpha|_{t_n} + \overbrace{\tau\left[1-\tau\ \underline{\underline{\left.\frac{\partial G_\alpha}{\partial \eta_\alpha}\right|_{t_n}}}\right]^{-1}}^{\underline{\underline{\mathcal{F}}}(\tau)} \underline{\underline{\left.\frac{\partial G_\alpha}{\partial \varphi}\right|_{t_n}}}\ \mathcal{B}[\mathring{\boldsymbol{\delta}}\boldsymbol{\varphi}] \\ \mathcal{B}[\mathring{\boldsymbol{\delta}}\boldsymbol{\varphi}] = \sum_\beta \underline{\underline{\left.\frac{\partial f}{\partial \eta_\beta}\right|_{t_n}}}\ \mathcal{B}[\mathring{\boldsymbol{\delta}}\boldsymbol{\eta}_\beta] + \underline{\underline{\left.\frac{\partial f}{\partial \varphi}\right|_{t_n}}}\ \mathcal{B}[\mathring{\boldsymbol{\delta}}\boldsymbol{\varphi}] \end{array} \right. \quad \text{(A-6)}$$

If the cell variables $\mathring{\boldsymbol{\delta}}\boldsymbol{\eta}$ are eliminated from the second equation, the complete system of equations (which includes cells) becomes:

$$\left\{ \begin{array}{c} \mathcal{B}[\mathring{\boldsymbol{\delta}}\boldsymbol{\eta}] = \mathcal{B}[\mathring{\boldsymbol{\delta}}\boldsymbol{\eta}_{dec}] + \underline{\underline{\mathcal{F}}}\,\mathcal{B}[\mathring{\boldsymbol{\delta}}\boldsymbol{\varphi}] \\ \left[1+\underline{\underline{\mathcal{C}}}\right]\mathcal{B}[\mathring{\boldsymbol{\delta}}\boldsymbol{\varphi}] = \mathcal{B}[\mathring{\boldsymbol{\delta}}\boldsymbol{\varphi}_{ins}] \end{array} \right. \quad \text{(A-7)}$$

where the quantities $\mathcal{B}[\mathring{\boldsymbol{\delta}}\boldsymbol{\eta}_{dec}]$, $\underline{\underline{\mathcal{F}}}$, $\underline{\underline{\mathcal{C}}}$, $\mathcal{B}[\mathring{\boldsymbol{\delta}}\boldsymbol{\varphi}_{ins}]$ depend on τ and can be calculated from the elementary Jacobian matrices and vectors at time t_n.

The first equation of (A-7) describes the evolution of the state variables. The state variables evolve because: (i) of their internal inertial evolutions $\mathring{\boldsymbol{\delta}}\boldsymbol{\eta}_{dec}$ (which would be obtained if transfer models were changed to constant transfer model with $\mathring{\boldsymbol{\delta}}\boldsymbol{\varphi} = \mathbf{0}$) ; (ii) of the evolution of their boundary conditions ($\mathring{\boldsymbol{\delta}}\boldsymbol{\varphi} \neq \mathbf{0}$). The matrix $\underline{\underline{\mathcal{F}}}$ describes the influence of transfer variables on state variables, and independently of the type of model used for these transfers ($\underline{\underline{\mathcal{F}}}$ is independent of the model of $\mathring{\boldsymbol{\delta}}\boldsymbol{\varphi}$).

In the second equation, $\mathring{\boldsymbol{\delta}}\boldsymbol{\varphi}_{ins}$ represents the variation of transfer variables if $\mathring{\boldsymbol{\delta}}\boldsymbol{\eta} = \mathring{\boldsymbol{\delta}}\boldsymbol{\eta}_{dec}$ (*i.e.* if the cell models were changed to decoupled models with $\underline{\underline{\mathcal{F}}} = 0$). Consequently, $\underline{\underline{\mathcal{C}}}$ represents the effect of cell and transfer coupling.

The developed expression of the matrix $\underline{\underline{\mathcal{C}}}$ shows how the partial derivatives defined at the cell and transfer level combine. The coefficients of the coupling matrix are rational fractions of the variable τ. This is the way the full dynamic of the system bounds the remaining variables after an algebraic elimination process.

b. Numerical solution of the Transfer Evolution Formalism

For large systems, the above matrices are huge and sparse, and exhibit an internal structure that depends upon the connections between cells and transfers. The full algorithm of the ZOOM[1] solver follows a technique called "relaxed super-nodes hyper multi-frontal method" (cf. Liu (1992)). We focus here on the principles of the resolution that explain how the system dynamics is described by the coupling coefficients.

Equivalence between Borel transform and the Crank-Nicolson scheme

It is easily shown that the Crank-Nicolson resolution of the system (A-4) with a time step δt, is identical to its Borel transform (A-7), with the correspondence $\tau \longleftrightarrow \frac{\delta t}{2}$.

To demonstrate this equivalence, let $\hat{\delta} X$ be the time evolution of variable X approximated by a Crank-Nicolson scheme, and consider the linear system:

[1] ZOOM is a TEF dedicated solver developed by the authors and colleagues.

$$\frac{\partial \eta(t)}{\partial t} = A \cdot \eta(t) \tag{A-8}$$

If $\eta(t) = \eta_0 + \delta\eta(t)$, with $\delta\eta(0) = 0$, it may be rewritten as:

$$\frac{\partial(\eta_0 + \delta\eta(t))}{\partial t} = A \cdot (\eta_0 + \delta\eta(t)) \tag{A-9}$$

If a Crank-Nicolson scheme is applied to the system (A-9), with a time step δt, the discretized equation reads:

$$\frac{\hat{\delta}\eta(\delta t)}{\delta t} = A\frac{1}{2}(2\eta_0 + \hat{\delta}\eta(\delta t)) \tag{A-10}$$

which gives the time evolution of η, since $\hat{\delta}\eta(\delta t) \approx \delta\eta(\delta t)$ for small δt.
For any $t > 0$, $\hat{\delta}\eta(t)$ is given by:

$$\hat{\delta}\eta(t) = \left(1 - \frac{t}{2}A\right)^{-1} A\eta_0 \cdot t \tag{A-11}$$

Now, the Borel transform of the system (A-9) reads:

$$\mathcal{B}\left(\frac{\partial \delta\eta}{\partial t}\right)(\tau) = \frac{1}{\tau}\mathcal{B}(\delta\eta)(\tau) = \mathcal{B}(A \cdot (\eta_0 + \delta\eta(t))) = A\mathcal{B}(\eta_0) + A\mathcal{B}(\delta\eta)(\tau) \tag{A-12}$$

which can be rewritten (because $\mathcal{B}(k) = k$ for a constant function k) as:

$$\mathcal{B}(\delta\eta)(\tau) = (1 - \tau A)^{-1} A\eta_0\tau \tag{A-13}$$

Equations (A-11) and (A-13) show that the Crank-Nicolson integration of a linear system is equivalent to the Borel transform of the system, through the relationship:

$$\hat{\delta}\eta(t) = 2 \cdot \mathcal{B}(\delta\eta)(\frac{t}{2}) \tag{A-14}$$

Time evolution of the model

For each time step, the ZOOM solver solves the second matrix equation of (A-7) for $\mathcal{B}[\mathring{\delta}\varphi]$. The first equation is then solved for $\mathcal{B}[\mathring{\boldsymbol{\delta}}\boldsymbol{\eta}]$. Thanks to the property (A-14), this gives an approximation of the temporal evolution of the model variables between t_n and $t_n + \delta t$.

TLS Analysis

As is well known, poles of Laplace transform of TLS solutions are eigenmodes of the system. The same holds for Borel transform: determining the poles of the Borel transform yields the complete dynamic of the system.

ZOOM is able to compute numerically the Borel transform of the TLS solution ($\mathcal{B}[\mathring{\boldsymbol{\delta}}\boldsymbol{\eta}](\tau)$ and $\mathcal{B}[\mathring{\boldsymbol{\delta}}\boldsymbol{\varphi}](\tau)$) on the real axis $\tau > 0$. The problem of describing the dynamics of a system is thus reduced to that of determining the poles of the Borel transform of the TLS solution from its numerical values on the positive real axis.

In particular, in Eq. (A-7), the poles of $\mathcal{B}[\mathring{\delta}\varphi](\tau)$ are (i) the poles of $\mathcal{B}[\mathring{\delta}\varphi_{ins}]$, i.e. the poles of the model without taking into account the interactions between sub-systems; (ii) the poles of $(1+\underline{\underline{C}})^{-1}$, i.e. the poles corresponding to the sub-system interaction. The inverse Borel transform of Eq. (A-7), obtained by an identification of simple elements, provides the full dynamics of the model. The methodology consists here in fitting the Borel transform with a linear combination of sigmoid and bump functions, which are the only possible Borel transforms of linear differential equation solutions. From the characteristic times of the corresponding poles and their residue, the original function can easily be reconstructed without inverse Borel transform.

References

Aires, F. and W. Rossow: 2003, Inferring instantenous, multivariate and nonlinear sensitivities for the analysis of feedback processes in a dynamical system: Lorenz model case study. *Quart. J. R. Met. Soc.*, **129**, 239–275.

Barsugli, J. and D. Battisti: 1998, The basic effects of atmosphere-ocean thermal coupling on midlatitude variability. *J. Atmos. Sci.*, **55**, 477–493.

Bates: 2003, On the ventilation feedback.

Cherkaoui, M., J. Dufresne, R. Fournier, J. Grandpeix, and A. Lahellec: 1996, Monte-Carlo simulation of radiation in gases with a narrow-band model and a net-exchange formulation. *J. Heat Tranfert*, **118**, 401–407.

Coakley, J.: 1977, Feedbacks in vertical-column energy balance models. *J. Atmos. Sci.*, **34**, 465–470.

Colman, R., S. Power, and B. McAvaney: 1997, Non-linear climate feedback analysis in an atmospheric general circulation model. *Climate Dynamics*, **13**, 717–731.

Del Genio, A., W. Kovari Jr, and M.-S. Yao: 1994, Climatic implications of the seasonal variation of upper tropospheric water vapor. *Geophysical Research Letters*, **21**, 2701–2704.

Goodman, J. and J. Marshall: 2003, Using neutral singular vectors to study low-frequency atmospheric variability (in press). *J. Atmos. Sci.*.

Green, J.: 1967, Division of radiative streams into internal tranfer and cooling to space. *Q. J. Roy. Meteor. Soc.*, **93**, 371–372.

Hall, A. and S. Manabe: 2000a, Effect of water vapor feedback on internal and anthropogenic variations of the global hydrologic cycle. *Journal of Geophysical Research*, **105**, 6935–6944.

— 2000b, Suppression of enso in a coupled model without water vapor feedback. *Climate Dynamics*, **16**, 393–403.

Hansen, J., D. Lacis, D. Rind, G. Rusell, P. Stone, I. Fung, R. Ruedy, and J. Lerner: 1984, Climate Sensitivity: Analysis of Feedback Mechanisms. *Climate Processes and Climate Sensitivity*, J. Hansen and T. Takahashi, eds., Geophysical monograph 29, AGU, volume 5, 130–162.

Hartmann, J. M., R. Levi Di Leon, and J. Taine: 1984, Line-by-Line and Narrow-Band Statistical Model Calculations for H_2O. *Journal of Quantitative Spectroscopy and Radiative Transfer*, **32**, 119–127.

Hu, Y. and K. Tung: 2002, Interannual and Decadal variations of planetary wave activity, stratospheric cooling, and northern hemisphere annular mode. *Journal of Climate*, **15**, 1659–1673.

IPCC: 2001, Climate Change 2001 : The Scientific Basis [J.T. Houghton, Y. Ding, D.J. Griggs, M. Noguer, P.J. Van der Linden, X. Dai, K. Maskell, C.A. Johnson] . *Cambridge University Press, Cambridge, United Kingdom and New-York, NY, USA, 880pp*.

Kothavala, Z., R. Oglesby, and B. Saltzman: 1999, Sensitivity of the equilibrium surface temperature of CCM3 to systematic changes in atmospheric carbon dioxyde. *Geophysical Research Letters*, **26**, 209–212.

Lindzen, S.: 1993, Climate dynamics and global change. *Annu. Rev. Fluid Mech.*, **26**, 353–378.

Liu, J. W. H.: 1992, The multifrontal method for sparse matrix solution: Theory and Practice. *Society for Industrial and Applied Mathematics Review*, **34**, 82–109.

Salathé, E. and D. Hartmann: 1997, A trajectory analysis of tropical upper-tropospheric moisture and convection. *Journal of Climate*, **10**, 2533–2547.

Salby, M.: 1996, Fundamentals of atmospheric physics,international geophysics series, academic press, san diego, california, united-states, 626 pp.

Schneider, E., B. Kirtman, and R. Lindzen: 1999, Upper tropospheric water vapor and climate sensitivity. *J. Atmos. Sci.*, **56**, 1649–1658.

Soufiani, A., J. M. Hartmann, and J. Taine: 1985, Validity of Band-Model Calculations for CO_2 and H_2O Applied to Radiative Properties and Conductive-Radiative Transfer. *Journal of Quantitative Spectroscopy and Radiative Transfer*, **33**, 243–257.

Wetherald, R. and S. Manabe: 1988, Cloud feedback processes in a general circulation model. *J. Atmos. Sci.*, **45**, 1397–1416.

Zhang, M., J. Hack, J. Kiehl, and R. Cess: 1994, Cloud feedback processes in a general circulation model. *Journal of Geophysical Research*, **99**, 5525–5537.